

DISCO: DIVERSIFYING SAMPLE CONDENSATION FOR EFFICIENT MODEL EVALUATION

CATCH, ADAPT, AND OPERATE: MONITORING ML MODELS UNDER DRIFT (CAO @ ICLR 2026)

Alexander Rubinstein¹ Benjamin Raible¹ Martin Gubri² Seong Joon Oh¹

¹Tübingen AI Center, University of Tübingen
²Parameter Lab

 [Project Page](#)  [DISCO Codebase](#)

ABSTRACT

To catch or avoid drift in deployed and in-development models we need to evaluate them as often as possible. For modern models, a single training run can produce hundreds of checkpoints, e.g., OLMo 2-32B has 753 on Hugging Face. Evaluating each of these checkpoints is currently impossible because even a single full evaluation becomes prohibitively expensive. Benchmarks such as LMMs-Eval and HELM demand thousands of GPU hours per model. To address the growing cost of standard evaluation, new methods focused on efficient evaluation have started to appear. The typical approach follows two steps. First, select an anchor subset of data. Second, train a mapping from the accuracy on this subset to the final test result. The drawback is that anchor selection depends on clustering, which can be complex and sensitive to design choices. We argue that promoting diversity among samples is not essential; what matters is to select samples that *maximise diversity in model responses*. Our method, **Diversifying Sample Condensation (DISCO)**, selects the top-k samples with the greatest model disagreements. This uses greedy, sample-wise statistics rather than global clustering. The approach is conceptually simpler. From a theoretical view, inter-model disagreement provides an information-theoretically optimal rule for such greedy selection. **DISCO** shows empirical gains over prior methods, achieving state-of-the-art results in performance prediction across MMLU, Hellaswag, Winogrande, and ARC. By enabling cheap, repeatable performance estimation, **DISCO** supports **operating at scale**: reliable monitoring and comparison of many models with minimal compute, so that frequent checkpoint evaluation and drift detection become feasible during development and in deployed ML systems.

1 INTRODUCTION

Model evaluation is becoming increasingly costly. Models have grown in size, which makes each inference expensive. Recent scaling of test-time computation has further raised the cost per task. End-user requirements have also broadened, covering both the content of the output and its style (Wang et al., 2018; Liang et al., 2022; Kim et al., 2023; Zhang et al., 2024). As a result, evaluation on modern benchmarks often requires hundreds to thousands of GPU hours. For instance, LMMs-Eval can take between 30 and 1400 hours on 8×A100 GPUs (Zhang et al., 2024). HELM requires more than 4000 GPU hours (Liang et al., 2022). In settings where ML systems must be **monitored under drift**—new data, new model variants, or shifting user populations—frequent re-evaluation is necessary but prohibitively expensive at full scale, motivating efficient evaluation methods that support **reliability at scale**.

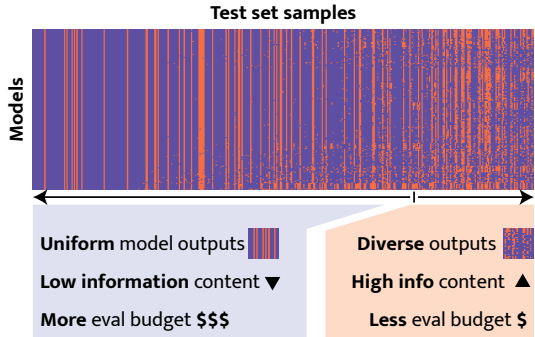


Figure 1: **Imbalance**. More evaluation budget is spent on less informative samples in test sets.

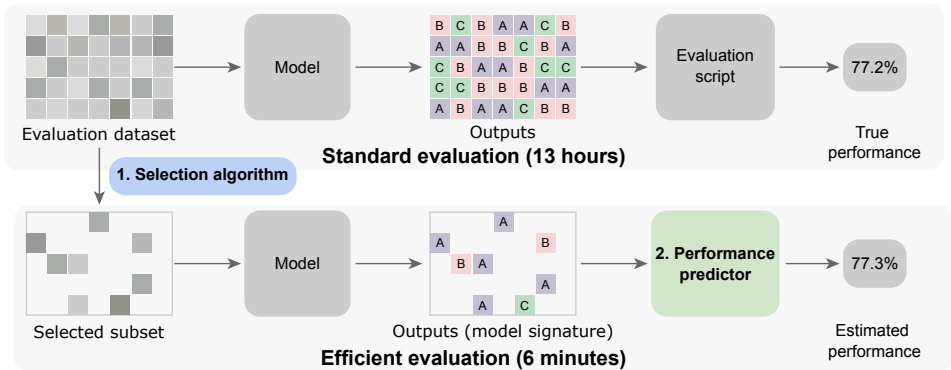


Figure 2: **Problem overview.** We aim at selecting a much smaller evaluation dataset than the original evaluation dataset, while keeping the estimated performances as close as possible. Figure 3 details the selection algorithm and the performance predictor.

Several efficient evaluation approaches have emerged. A common framework works in two parts: subset selection and performance prediction. The first part selects a static subset of anchor points from the evaluation dataset. The second part predicts full benchmark performance by extrapolating from accuracy on this subset. To select anchor points, existing methods often rely on clustering. Samples are grouped by the similarity of responses they induce in a set of reference models (Vivek et al., 2023; Polo et al., 2024). Variants of this framework include dynamic anchor selection (Hofmann et al., 2025), modified prediction models (Kipnis et al., 2024), and new benchmarks for method comparison (Zhang et al., 2025).

We seek to improve both parts of this framework. For subset selection, we argue that diversity among samples is not essential. What matters is **diversity in model responses**. We prove that inter-model disagreement is the most informative signal for estimating benchmark performance when the goal is to differentiate and rank models (Proposition 1). Evaluation should therefore focus on samples that elicit varied responses (Figure 1). For performance prediction, we argue that existing methods add unnecessary complexity by estimating hidden model parameters before predicting test performance (Polo et al., 2024; Kipnis et al., 2024). We instead propose a direct route. Model signatures, defined as the concatenation of outputs on the selected subset, serve as inputs to simple predictors of benchmark performance. This framework is simpler, yet matches and surpasses more complex alternatives.

We validate these ideas through **Diversifying Sample Condensation (DISCO)**. DISCO selects a small, informative subset of evaluation samples by focusing on model disagreement. Disagreement is measured by predictive diversity scoring (PDS, Rubinstein et al. (2024)), originally proposed for out-of-distribution detection. A simple metamodel then predicts benchmark performance directly from the model signatures on this subset. We evaluate DISCO in both language and vision domains. On MMLU, for example, DISCO reduces evaluation cost by 99.3% (see § C.4) with only 1.07 percentage points of error. Compared with prior methods such as Anchor Points (Vivek et al., 2023), TinyBenchmarks (Polo et al., 2024), and Metabench (Kipnis et al., 2024), DISCO achieves a stronger efficiency-precision trade-off.

Relevance to CAO. This work aligns with the workshop’s theme of *Operating at Scale*: it provides systems-friendly, cost-effective evaluation so that many models can be monitored and compared with minimal compute. Model signatures and disagreement-based selection also support *representation-based monitoring*: compact, informative summaries of model behaviour that can signal when new or updated models diverge from expectations.

Related work is deferred to Appendix A.

2 PROBLEM

Our task is the estimation of model performance on a benchmark. Let $f : \mathcal{X} \rightarrow \mathcal{Y}$ be a predictive model over a dataset $\mathcal{D} := \{(x_1, y_1), \dots, (x_N, y_N)\}$ sampled iid from some distribution. We are

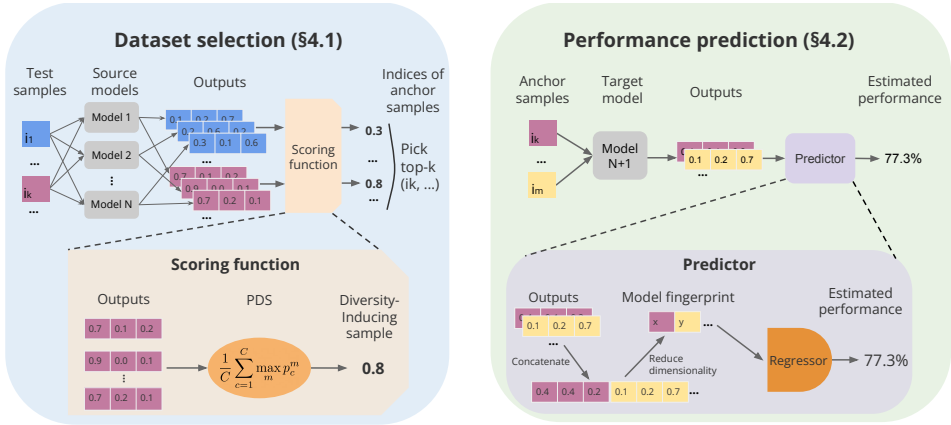


Figure 3: **DISCO overview**. First, we select a subset of an evaluation dataset with the most informative samples. Second, we predict the performance of unseen models from their outputs on the selected samples.

interested in estimating the model performance on the dataset $r(f, \mathcal{D})$. An example metric for model performance is accuracy: for a probabilistic classifier $f : \mathcal{X} \rightarrow [0, 1]^C$, accuracy is defined as $\frac{1}{N} \sum_i \mathbf{1}(\arg \max_c f_c(x_i) = y_i)$.

We are interested in estimating $r(f, \mathcal{D})$ in a cost-effective way. We seek ways to sample a subset of size $K \ll N$ from the original set \mathcal{D} to estimate $r(f, \mathcal{D})$. The overall problem is described in Figure 2. An integral ingredient for both prior works and ours is the set of *source models* $\mathcal{F} = \{f^1, \dots, f^M\}$, a held-out set of models whose ground-truth performances are known. We define the *target models* as the models whose performances we aim to estimate.

3 SOLUTION

This section presents DISCO, our solution to the problem of efficient performance evaluation. DISCO is composed of two steps: (i) the dataset selection, where given an original dataset and an held-out set of source models, we identify a much smaller subset of samples; and (ii) the performance prediction, where given the model outputs on our DISCO selected evaluation set, we estimate the model performance on the original set.

3.1 DATASET SELECTION

At this stage, we require a score that quantifies each sample’s informativeness for predicting performance on the full dataset. Using this score, we rank the samples and select a top-k subset that best preserves the dataset’s information content.

3.1.1 PRIOR SELECTION METHODS

We first review existing approaches for selecting representative data points in the evaluation set, referred to as anchor points.

Anchor-conf Vivek et al. (2023) choose K anchors $A = \{a_k\}_1^K \subset \{x_i\}_1^N$ that minimise the sum of distances between each data point and the closest anchor: $\min_A \sum_{i,k} d(e(x_i), e(a_k))$, where the $e(x)$ abbreviates the concatenated model likelihoods $e(x, y) := [f^1(x)_y, \dots, f^M(x)_y]$ for the input and ground-truth label (x, y) for the source models $\mathcal{F} = \{f^1, \dots, f^M\}$.

Anchor-corr (Polo et al., 2024) is nearly identical to *Anchor-conf*, except that the embedding uses correctness scores instead of likelihoods: $e(x, y) := \{s^1(x, y), \dots, s^M(x, y)\}$, where $s^m(x, y) := \mathbf{1}(\arg \max_c f^m(x)_c = y)$ encodes correctness of model f^m on sample x .

Anchor-IRT (Polo et al., 2024) uses the Item-Response Theory (IRT) to define a parametric model $\Pr(s_i^m = 1 \mid \theta^m, \alpha_i, \beta_i) = \text{sigmoid}(-\alpha_i^\top \theta^m + \beta_i)$. It predicts the correctness of a model f^m on

a sample x_i with parameters $\theta^m \in \mathbb{R}^d$, $\alpha_i \in \mathbb{R}^d$, and $\beta_i \in \mathbb{R}$. Using observations of the sample-wise correctness of source models (x_i, y_i, s_i^m) , the parameters are inferred with an Expectation-Maximisation algorithm. Now, they continue the anchor selection based on the sample-wise embeddings $e(x_i) := (\alpha_i, \beta_i)$.

Best for validation Kipnis et al. (2024) finds an anchor set A through an iterative search. The algorithm first generates a large number of candidate anchor sets, $\{A_1, \dots, A_P\}$, by uniformly sampling from the full dataset \mathcal{D} . For each candidate set A_p , a simple scalar-to-scalar regression model, g_p , is trained on the source models \mathcal{F} . This model learns to map the performance on the subset, $r(f, A_p)$, to the known ground-truth performance on the full dataset, $r(f, \mathcal{D})$. Each trained regressor g_p is subsequently evaluated on a held-out validation set of models. The final anchor set A is selected as the candidate A_p whose corresponding regressor g_p yields the lowest prediction error (e.g., RMSE) on this validation set.

How DISCO differs. Unlike clustering, we use sample-wise statistic to determine samples with maximal information content. This greatly simplifies the sampling procedure. We exploit the **model diversity**, not **model confidence** or **correctness**. A set of models can be highly confident and diverse at the same time. We argue that inputs that induce model diversity are more useful for performance prediction.

3.1.2 DISCO SELECTION

We now present our selection method. In this part, we explain how we identify such samples in the test dataset. Our sample selection strategies are illustrated in Figure 3. The main approach in **Diversifying Sample Condensation (DISCO)** is to select a subset $\mathcal{D}_{\text{DISCO}}$ of the original evaluation set \mathcal{D} by sampling the top-k samples based on disagreement score, such as PDS. This follows the intuition shown in Figure 1.

We start with an information-theoretic observation below.

Proposition 1. Let $\mathcal{D} = \{(x_i, y_i)\}_i^N$ be a test set and $m \sim \text{Unif}\{1, \dots, M\}$ (A1) be the index of a uniformly chosen model. Let $f_c^m(x_i) \in [0, 1]$ be the predictive probability for class c of model f^m on input x_i . We write \hat{y}_i^m for the categorical random variable following $\text{Cat}(f_1^m(x_i), \dots, f_C^m(x_i))$. Define ensemble mean prediction to be $\bar{f}_c(x_i) := \mathbb{E}_m[f_c^m(x_i)]$ for each class c and define corresponding prediction random variable as \hat{y}_i following $\text{Cat}(\bar{f}_1(x_i), \dots, \bar{f}_C(x_i))$. Let $S(m) = S(f^m, \mathcal{D})$ denote a function of model m and dataset \mathcal{D} , such as model accuracy, that is injective with respect to m . Assume that the only randomness in \hat{y}_i^m comes from m (A2). Then,

$$\text{MI}_{m, \hat{y}_i}(S(m); \hat{y}_i) = H(\hat{y}_i) - \mathbb{E}_m[H(\hat{y}_i^m)] = \text{JSD}(\hat{y}_i^1, \dots, \hat{y}_i^M).$$

where $H(\cdot)$ is entropy, $\text{MI}(\cdot)$ is mutual information, and $\text{JSD}(\cdot)$ is generalised Jensen-Shannon Divergence for multiple distributions (Fuglede & Topsøe, 2004).

See proof in Appendix G.1.

We conclude that the sample i conveying the greatest level of information for the prediction of $S(m)$ (e.g. model accuracy) is the one with greatest JSD $(\hat{y}_i^1, \dots, \hat{y}_i^M)$. This generalised Jensen-Shannon divergence translates to the diversity of distributions (Fuglede & Topsøe, 2004). Based on the insight that model diversity matters for performance prediction, we also consider an alternative measure that measures the model diversity: predictive diversity score (PDS) (Rubinstejn et al., 2024). It is more interpretable, as it is a continuous generalisation of the number of unique argmax category predictions among M source models:

$$\text{PDS}(\hat{y}_i^1, \dots, \hat{y}_i^M) := \frac{1}{C} \sum_c \max_m f_c^m(x_i). \quad (1)$$

PDS is related to JSD through the enveloping inequalities below:

Proposition 2. Denoting $\text{PDS}_i := \text{PDS}(\hat{y}_i^1, \dots, \hat{y}_i^M)$, $\text{JSD}_i := \text{JSD}(\hat{y}_i^1, \dots, \hat{y}_i^M)$ for each sample i , we have

$$\frac{2}{M^2 \ln 2} (\text{PDS}_i - 1)^2 \leq \text{JSD}_i \leq \frac{M}{M-1} \log M \cdot (\text{PDS}_i - 1).$$

See proof in Appendix H.3.

In the experiments, we consider both JSD and PDS as criteria for sample selection.

3.2 PERFORMANCE PREDICTION

Once a subset of dataset samples A is selected, we use the responses of the target model f on A to estimate the true performance.

3.2.1 PRIOR PREDICTION METHODS

We first review existing approaches for estimating the true performance using predictions on anchor points $A = \{a_1, \dots, a_K\}$.

Weighted sum Vivek et al. (2023) estimates the true performance by directly computing the accuracy on the anchor set: $WS(f, A) := (1/K) \sum_k w_k s_k^m$, where w_k is the number of original training samples x_i assigned to the anchor a_k in the *Anchor-Corr* method.

p-IRT (Polo et al., 2024): makes adjustments to the vanilla accuracy on the anchor set by adding a correction term derived from the IRT in *Anchor-IRT* in: $p\text{-IRT}(f, A) := (1/K) \sum_{k \in A} s_k + 1/(N - K) \sum_{k \notin A} p_i$, where \hat{p}_i is the IRT estimation computed based on the parameters obtained in *Anchor-IRT*.

gp-IRT (Polo et al., 2024) is a mixture of the two approaches above: $gp\text{-IRT}(f, A) = \lambda \cdot WS(f, A) + (1 - \lambda) \cdot p\text{-IRT}(f, A)$ where $\lambda \in [0, 1]$.

ability-IRT Kipnis et al. (2024) is a two-stage method that uses the anchor set A as a diagnostic tool rather than just a miniature test. First, it uses a pre-calibrated IRT model to estimate a latent “ability” score, $\hat{\theta}^f$, from the target model’s pattern of correct and incorrect responses on A . Second, a pre-trained regressor, g , predicts the final performance S^f using both the simple anchor set accuracy \hat{S}_A^f and this more informative ability score $\hat{\theta}^f$ as input features. The final prediction is given by $S^f = g(\hat{S}_A^f, \hat{\theta}^f)$, leveraging a deeper measure of the model’s capability to improve the estimate.

How DISCO differs. Previous prediction methods rely on scalar summaries of performance, such as the (weighted or corrected) accuracy on the anchor set. In contrast, our approach leverages a much richer signal: the **model signature**, defined as the concatenation of the model’s raw outputs on the selected samples. By learning a direct mapping from the high-dimensional signature to the final performance, we bypass the complexities of psychometric modeling and demonstrate that a simpler, more direct approach can be more effective.

3.2.2 DISCO PREDICTION

Given a smaller set of test dataset $\mathcal{D}_{\text{DISCO}}$, we estimate the performance of a model f as closely as possible to the true full test performance $r(f, \mathcal{D})$. We deliberately opt for simple approaches here, in order to make a point that simple is best; we also compare against a rather complex prior work and show that our simple method outperforms it. Our performance prediction framework is depicted in Figure 3.

Model signatures. We hypothesise that models with similar output patterns on $\mathcal{D}_{\text{DISCO}}$ will exhibit similar performance. To capture this pattern, we define a **model signature** as the concatenation of the model’s outputs on $\mathcal{D}_{\text{DISCO}}$: $f(\mathcal{D}_{\text{DISCO}}) := [f(x_1), \dots, f(x_L)]$.

Such function signature may have a large dimensionality, as it is the product of model output dimensionality (e.g. 1000 for ImageNet) and the number of selected samples $|\mathcal{D}_{\text{DISCO}}|$ (e.g. can go up to 50k for ImageNet validation set). To reduce the storage burden and improve generalizability, we consider applying a dimensionality reduction technique based on principal component analysis (PCA): $Q \circ f(\mathcal{D}_{\text{DISCO}})$.

KNN prediction. Built on the hypothesis that the similarities in function signature imply performance similarity, we consider the kNN predictor based on a held-out set of models \mathcal{F} . Given a function f to evaluate, we identify the K most similar models in \mathcal{F} using the Euclidean distance between their signatures after dimensionality reduction. We estimate f ’s performance by averaging the performances of the K most similar models.

Parametric mapping. We also consider a parametric prediction variant. A single parametric mapping R is trained for the prediction of model performance. As the training set, we use M model signatures $Q \circ f_1(\mathcal{D}_{\text{DISCO}}), \dots, Q \circ f_M(\mathcal{D}_{\text{DISCO}})$ for \mathcal{F} as the training set for the regression problem

of training a mapping $R(\cdot)$ to let $R \circ Q \circ f_m(\mathcal{D}_{\text{DISCO}})$ approximate $\hat{r}(f, \mathcal{D})$. The predictor R can be implemented using a neural network, linear regression, or a Random Forest, for example.

4 EXPERIMENTS

In this section, we introduce the experimental setup (§4.1), present the main results of Diversifying Sample Condensation (DISCO) in language domain (§4.2), analyse contributing factors (§B.1), and demonstrate that the method is domain-agnostic and can also be successfully applied to the vision domain (Appendix I).

4.1 SETUP

In this section we describe our experimental setup: used datasets, models, model splits, metrics, and evaluation protocol.

Datasets. We evaluate DISCO on four widely used language modeling benchmarks: MMLU (Hendrycks et al., 2021), HellaSwag (Zellers et al., 2019) Winogrande (Sakaguchi et al., 2021), and ARC (Clark et al., 2018). Details on the benchmarks can be seen in § B.

Models. Building on the TinyBenchmarks framework (Polo et al., 2024), we evaluate 424 large language models (LLMs) from Hugging Face’s Open LLM Leaderboard (Fourrier et al., 2024). The models cover GPT- (Radford et al., 2019), LLaMA- (Touvron et al., 2023), DeepSeek- (DeepSeek-AI et al., 2025), and BERT-style (Devlin et al., 2019) architectures, with model sizes ranging from 1.3 billion to 72 billion parameters.

Model split. DISCO is based on a meta-model approach where a predictor is constructed based on the model signatures of a pool of source models \mathcal{F} and tested on a disjoint set of target models. This approach has traditionally been criticised for its dependency on the set of existing models: the predictor may fail to retain performance with unforeseen changes in future models. To address this concern, we introduce the *chronological split*, where the source models \mathcal{F} consist of models published before January 13, 2024 and the meta test set consists of models after the cutoff date. The train-test ratio is 9:1.

Metrics. We evaluate DISCO and baseline approaches using two complementary metrics. First, the Mean Absolute Error (*MAE*) of the model accuracies, reported as percentage points (%p), captures the absolute error of accuracy prediction. Second, to assess the consistency of the relative ordering of models, we report the Spearman rank correlation (*Rank*) in model ranking between the true and estimated model performances.

Evaluation. Following the overview of the solution to the efficient evaluation problem in § 3, our protocol for evaluating methods looks as follows:

Training.

- Input: source models \mathcal{F} , full test dataset \mathcal{D} , parameter K .
 - Output: set of anchor datapoints A_K , predictor.
1. Evaluate source models \mathcal{F} on full test dataset \mathcal{D} .
 2. Calculate performance $S_{\mathcal{F}}$ of source models on the full test dataset.
 3. Use model outputs from the previous steps and optionally ground truth labels to select a set A_K of K anchor datapoints with respective selection method (PDS/JSD, IRT, etc) explained in § 3.1.
 4. Train respective predictor (Random Forest, gp-IRT, ability-IRT, etc) explained in § 3.2.2 to predict $S_{\mathcal{F}}$ from outputs of source models \mathcal{F} on A_K .

Testing:

- Input: target model (or test set of target models), set of anchor points A_K , predictor, ground truth performance S of target model on \mathcal{D} .
- Output: performance of efficient evaluation method.

| Approach | Selection | Prediction | MMLU (14k) | | HS (10k) | | WG (1.3k) | | ARC (1.2k) | |
|-----------------|---------------|--------------|-------------|--------------|--------------|--------------|-------------|--------------|--------------|---------------|
| | | | §3.1 | §3.2 | MAE↓ Rank↑ | MAE↓ Rank↑ | MAE↓ Rank↑ | MAE↓ Rank↑ | MAE↓ Rank↑ | |
| Baseline | Random | Direct eval. | 3.45 | 0.916 | 2.85 | 0.839 | 3.60 | 0.827 | 2.61 | 0.898 |
| tinyBenchmarks | Random | gp-IRT | 2.79 | 0.922 | 1.96 | 0.819 | 1.64 | 0.928 | 2.22 | 0.921 |
| | Anchor-IRT | gp-IRT | 3.25 | 0.922 | 2.19 | 0.830 | 2.24 | 0.850 | 4.55 | 0.708 |
| | Anchor-corr | gp-IRT | 2.08 | 0.927 | 1.27 | 0.937 | 1.95 | 0.918 | 2.18 | 0.948 |
| metaBench | Best for val. | ability-IRT | 2.08† | 0.904† | 0.80† | 0.974† | 1.23† | 0.947† | 1.14† | 0.971† |
| Model signature | Random | Sig. + kNN | 1.82 | 0.912 | 1.49 | 0.899 | 1.58 | 0.920 | 2.30 | 0.905 |
| | | Sig. + RF | 1.81 | 0.933 | 1.36 | 0.938 | 1.29 | 0.926 | 1.72 | 0.938 |
| DISCO (ours) | High PDS | Sig. + kNN | 1.31 | 0.972 | 1.32 | 0.956 | 1.19 | 0.951 | 1.96 | 0.937 |
| | | Sig. + RF | 1.07 | 0.987 | 1.01 | 0.984 | 1.00 | 0.967 | 1.47 | 0.971 |
| | High JSD | Sig. + kNN | 1.14 | 0.975 | 1.50 | 0.944 | 1.26 | 0.955 | 2.11 | 0.939 |
| | | Sig. + RF | 1.30 | 0.987 | 0.86 | 0.972 | 1.09 | 0.973 | 1.75 | 0.938 |

Table 1: **DISCO achieves state-of-the-art test-set compression by using model signatures combined with PDS for accurate performance prediction.** Compression of MMLU, HellaSwag (HS), Winogrande (WG) and ARC datasets by DISCO (ours), tinyBenchmarks, metaBench and other baselines. For each dataset, we reduce the test set to 100 data points (except for metaBench, see below), achieving inference cost reduction of 99.3% and 99.0%, on MMLU and HS, respectively. Sig. + RF/kNN stands for model signature with Random Forest/kNN prediction (§ 3.2.2). Mean absolute error (MAE) is the %p difference in accuracy, and Rank is the Spearman rank correlation between the true model ranking and the estimated model ranking. † Results for metaBench are not directly comparable, as it requires more examples to converge: 150 datapoints for MMLU and ARC (+50%), 450 for HS (+350%), and 200 for WG (+100%). See § E for confidence intervals.

1. Evaluate target model on anchor points A_K .
2. Use predictor to estimate \hat{S} performance of the target model on \mathcal{D} from its outputs on A_K .
3. Calculate performance of efficient evaluation method based on S and \hat{S} .

4.2 MAIN RESULTS

Table 1 shows the main results. Uniform random sampling, together with direct evaluation with the corresponding annotated labels, yields 3.45%p MAE and .916 rank correlation at 100 samples. The approaches introduced in tinyBenchmarks Polo et al. (2024) improve over this baseline, confirming their findings.

We measure the efficacy of DISCO in two steps: adopt model-signature approach on top of uniform random sample selections first, and then consider sampling according to predictive diversity scoring (PDS). Even without PDS, on uniform random samples, model signatures are achieving 1.81%p MAE and .933 rank correlation with Random Forest (RF), reaching the state-of-the-art performance with simple and practical ingredients. When PDS is further considered for sample selection, to diversify the model outputs, we achieve 1.07%p MAE and .987 rank correlation (see § D for qualitative comparison of predicted ranks for DISCO vs direct evaluation), demonstrating a significant leap from the prior state of the art from tinyBenchmarks Polo et al. (2024) from ICML 2024.

To provide an understanding of the distributional comparison of the true model performances and the estimated performances, we show a scatter plot in Figure 4. As signified by the high Pearson’s correlation coefficient at .986, the estimated performances closely follow the true performances.

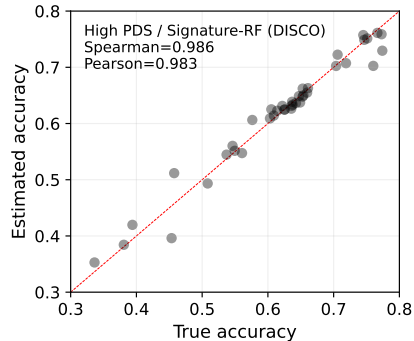


Figure 4: **True and estimated performance on MMLU.** Scatter plot of performances of 40 models.

Figure 5 shows the performance against varying degrees of the test set reduction. We observe that the ranking of estimated evaluation methodologies does not change much across a wide range of degrees of reduction. In particular, our DISCO is consistently the best method across all ranges

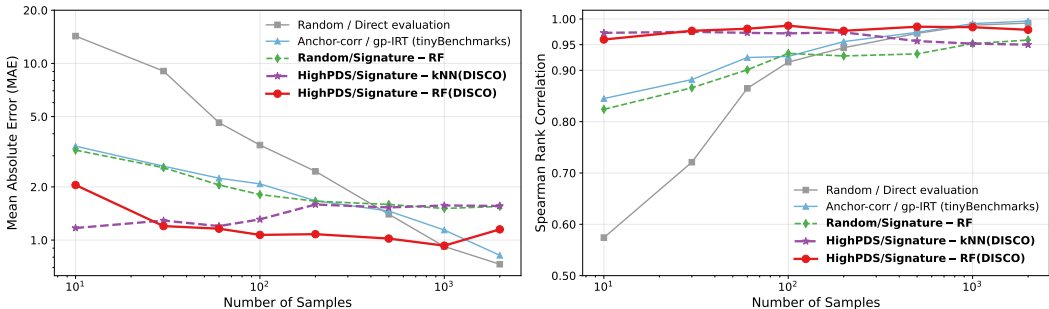


Figure 5: **MMLU performance estimation vs. compression rates.** Mean absolute error (MAE), measured in %p difference in accuracy, and the Spearman rank correlation between the true model ranking and the estimated model ranking are shown. At 100 samples, the results are identical to Table 1. **Main observations:** DISCO hits a better efficiency-precision trade-off across all range of compression rates. For extreme compression rate, kNN is a better choice than random forest (RF).

of number of samples involved. For the extreme rates of compression, at 10 samples, the non-parametric performance predictor of kNN yields better performance than the parametric Random Forest, suggesting that non-parametric approaches may be more suitable at extreme compression.

Factor analysis (model split, stratification, number of source models, dimensionality reduction, prediction model) is deferred to Appendix B.1.

We also evaluate DISCO on the vision domain (ImageNet-1k); see Appendix I for setup, baselines, and full results.

5 CONCLUSION

Evaluating ML models is increasingly expensive due to larger models, datasets, and benchmarks. It is especially true for general-purpose LLMs requiring broad evaluation.

We propose DISCO, which selects a small informative subset of the evaluation data and estimates model performance from predictions on it. DISCO cuts evaluation costs by over 99% with minimal error and consistently outperforms prior methods.

This enables practical use: efficient evaluation on limited compute, frequent performance tracking during training, and cheap end-user checks of deployed models.

Limitations. The main limitation of DISCO is robustness to distribution shifts in the model population. Shifts can arise from new architectures, training methods, or objectives, introducing patterns unseen during training and reducing estimator accuracy. Addressing this aligns with the CAO theme of *Responding to Drift*: future work could combine DISCO with adaptive sample selection or periodic retraining on newer models to maintain reliable monitoring under drift.

We also note unsuitable tasks for DISCO. The main constraint is that DISCO requires predictive probabilities for several predefined answer choices for each question (the classes in Proposition 1). That makes DISCO not suitable for open-ended generation tasks such as translation or summarization. Applying DISCO to such tasks would first require defining sets of correct and incorrect outputs. We leave such experiments for future work.

REFERENCES

Peter Clark, Isaac Cowhey, Oren Etzioni, Tushar Khot, Ashish Sabharwal, Carissa Schoenick, and Oyvind Tafjord. Think you have solved question answering? try arc, the ai2 reasoning challenge. *arXiv preprint arXiv:1803.05457*, 2018. 6, 14

DeepSeek-AI, Daya Guo, Dejian Yang, Haowei Zhang, Junxiao Song, Ruoyu Zhang, Runxin Xu, Qihao Zhu, Shirong Ma, Peiyi Wang, Xiao Bi, Xiaokang Zhang, Xingkai Yu, Yu Wu, Z. F. Wu, Zhibin Gou, Zhihong Shao, Zhuoshu Li, Ziyi Gao, Aixin Liu, Bing Xue, Bingxuan Wang, Bochao

- Wu, Bei Feng, Chengda Lu, Chenggang Zhao, Chengqi Deng, Chenyu Zhang, Chong Ruan, Damai Dai, Deli Chen, Dongjie Ji, Erhang Li, Fangyun Lin, Fucong Dai, Fuli Luo, Guangbo Hao, Guanting Chen, Guowei Li, H. Zhang, Han Bao, Hanwei Xu, Haocheng Wang, Honghui Ding, Huajian Xin, Huazuo Gao, Hui Qu, Hui Li, Jianzhong Guo, Jiashi Li, Jiawei Wang, Jingchang Chen, Jingyang Yuan, Junjie Qiu, Junlong Li, J. L. Cai, Jiaqi Ni, Jian Liang, Jin Chen, Kai Dong, Kai Hu, Kaige Gao, Kang Guan, Kexin Huang, Kuai Yu, Lean Wang, Lecong Zhang, Liang Zhao, Litong Wang, Liyue Zhang, Lei Xu, Leyi Xia, Mingchuan Zhang, Minghua Zhang, Minghui Tang, Meng Li, Miaojun Wang, Mingming Li, Ning Tian, Panpan Huang, Peng Zhang, Qiancheng Wang, Qinyu Chen, Qiushi Du, Ruiqi Ge, Ruisong Zhang, Ruizhe Pan, Runji Wang, R. J. Chen, R. L. Jin, Ruyi Chen, Shanghao Lu, Shangyan Zhou, Shanhuang Chen, Shengfeng Ye, Shiyu Wang, Shuiping Yu, Shunfeng Zhou, Shuting Pan, S. S. Li, Shuang Zhou, Shaoqing Wu, Shengfeng Ye, Tao Yun, Tian Pei, Tianyu Sun, T. Wang, Wangding Zeng, Wanxia Zhao, Wen Liu, Wenfeng Liang, Wenjun Gao, Wenqin Yu, Wentao Zhang, W. L. Xiao, Wei An, Xiaodong Liu, Xiaohan Wang, Xiaokang Chen, Xiaotao Nie, Xin Cheng, Xin Liu, Xin Xie, Xingchao Liu, Xinyu Yang, Xinyuan Li, Xuecheng Su, Xuheng Lin, X. Q. Li, Xiangyue Jin, Xiaojin Shen, Xiaosha Chen, Xiaowen Sun, Xiaoxiang Wang, Xinnan Song, Xinyi Zhou, Xianzu Wang, Xinxia Shan, Y. K. Li, Y. Q. Wang, Y. X. Wei, Yang Zhang, Yanhong Xu, Yao Li, Yao Zhao, Yaofeng Sun, Yaohui Wang, Yi Yu, Yichao Zhang, Yifan Shi, Yiliang Xiong, Ying He, Yishi Piao, Yisong Wang, Yixuan Tan, Yiyang Ma, Yiyuan Liu, Yongqiang Guo, Yuan Ou, Yudian Wang, Yue Gong, Yuheng Zou, Yujia He, Yunfan Xiong, Yuxiang Luo, Yuxiang You, Yuxuan Liu, Yuyang Zhou, Y. X. Zhu, Yanhong Xu, Yanping Huang, Yaohui Li, Yi Zheng, Yuchen Zhu, Yunxian Ma, Ying Tang, Yukun Zha, Yuting Yan, Z. Z. Ren, Zehui Ren, Zhangli Sha, Zhe Fu, Zhean Xu, Zhenda Xie, Zhengyan Zhang, Zhewen Hao, Zhicheng Ma, Zhigang Yan, Zhiyu Wu, Zihui Gu, Zijia Zhu, Zijun Liu, Zilin Li, Ziwei Xie, Ziyang Song, Zizheng Pan, Zhen Huang, Zhipeng Xu, Zhongyu Zhang, and Zhen Zhang. Deepseek-r1: Incentivizing reasoning capability in llms via reinforcement learning, 2025. URL <https://arxiv.org/abs/2501.12948>. 6
- Weijian Deng and Liang Zheng. Are labels always necessary for classifier accuracy evaluation? In *Proceedings of the IEEE/CVF conference on computer vision and pattern recognition*, pp. 15069–15078, 2021. 13
- Jacob Devlin, Ming-Wei Chang, Kenton Lee, and Kristina Toutanova. BERT: Pre-training of deep bidirectional transformers for language understanding. In Jill Burstein, Christy Doran, and Thamar Solorio (eds.), *Proceedings of the 2019 Conference of the North American Chapter of the Association for Computational Linguistics: Human Language Technologies, Volume 1 (Long and Short Papers)*, pp. 4171–4186, Minneapolis, Minnesota, June 2019. Association for Computational Linguistics. doi: 10.18653/v1/N19-1423. URL <https://aclanthology.org/N19-1423/>. 6
- Alexey Dosovitskiy, Lucas Beyer, Alexander Kolesnikov, Dirk Weissenborn, Xiaohua Zhai, Thomas Unterthiner, Mostafa Dehghani, Matthias Minderer, Georg Heigold, Sylvain Gelly, Jakob Uszkoreit, and Neil Houlsby. An image is worth 16x16 words: Transformers for image recognition at scale, 2021. URL <https://arxiv.org/abs/2010.11929>. 24, 25
- Riccardo Fogliato, Pratik Patil, Mathew Monfort, and Pietro Perona. A framework for efficient model evaluation through stratification, sampling, and estimation. In *European Conference on Computer Vision*, pp. 140–158. Springer, 2024. 13, 24, 25
- Clémentine Fourier, Nathan Habib, Alina Lozovskaya, Konrad Szafer, and Thomas Wolf. Open llm leaderboard v2. https://huggingface.co/spaces/open-llm-leaderboard/open_llm_leaderboard, 2024. 6
- B. Fuglede and F. Topsoe. Jensen-shannon divergence and hilbert space embedding. In *International Symposium on Information Theory, 2004. ISIT 2004. Proceedings.*, pp. 31–, 2004. doi: 10.1109/ISIT.2004.1365067. 4
- Vipul Gupta, Candace Ross, David Pantoja, Rebecca J. Passonneau, Megan Ung, and Adina Williams. Improving model evaluation using SMART filtering of benchmark datasets. In Luis Chiruzzo, Alan Ritter, and Lu Wang (eds.), *Proceedings of the 2025 Conference of the Nations of the Americas Chapter of the Association for Computational Linguistics: Human Language Technologies (Volume 1: Long Papers)*, pp. 4595–4615, Albuquerque, New Mexico, April 2025.

- Association for Computational Linguistics. ISBN 979-8-89176-189-6. doi: 10.18653/v1/2025.naacl-long.235. URL <https://aclanthology.org/2025.naacl-long.235/>. 13
- Dan Hendrycks, Collin Burns, Steven Basart, Andy Zou, Mantas Mazeika, Dawn Song, and Jacob Steinhardt. Measuring massive multitask language understanding. *Proceedings of the International Conference on Learning Representations (ICLR)*, 2021. 6, 14
- Valentin Hofmann, David Heineman, Ian Magnusson, Kyle Lo, Jesse Dodge, Maarten Sap, Pang Wei Koh, Chun Wang, Hannaneh Hajishirzi, and Noah A. Smith. Fluid language model benchmarking. In *Second Conference on Language Modeling*, 2025. URL <https://openreview.net/forum?id=mxCG9YRqj>. 2, 13
- Zhengyu Hu, Jieyu Zhang, Yue Yu, Yuchen Zhuang, and Hui Xiong. How many validation labels do you need? exploring the design space of label-efficient model ranking. *ArXiv*, abs/2312.01619, 2023. URL <https://api.semanticscholar.org/CorpusId:265610019>. 13
- Yuheng Huang, Jiayang Song, Qiang Hu, Felix Juefei-Xu, and Lei Ma. Active testing of large language model via multi-stage sampling. *arXiv preprint arXiv:2408.03573*, 2024. 13
- Disi Ji, Robert L Logan, Padhraic Smyth, and Mark Steyvers. Active bayesian assessment of black-box classifiers. In *Proceedings of the AAAI Conference on Artificial Intelligence*, pp. 7935–7944, 2021. 13
- Seungone Kim, Jamin Shin, Yejin Cho, Joel Jang, Shayne Longpre, Hwaran Lee, Sangdoon Yun, Seongjin Shin, Sungdong Kim, James Thorne, et al. Prometheus: Inducing fine-grained evaluation capability in language models. In *The Twelfth International Conference on Learning Representations*, 2023. 1, 13
- Alex Kipnis, Konstantinos Voudouris, Luca M. Schulze Buschoff, and Eric Schulz. metabench – a sparse benchmark of reasoning and knowledge in large language models. In *unknown*, 2024. URL <https://api.semanticscholar.org/CorpusId:271269996>. 2, 4, 5, 13
- Jannik Kossen, Sebastian Farquhar, Y. Gal, and Tom Rainforth. Active testing: Sample-efficient model evaluation. In *International Conference on Machine Learning*, 2021. URL <https://arxiv.org/pdf/2103.05331.pdf>. 13
- Jannik Kossen, Sebastian Farquhar, Yarin Gal, and Thomas Rainforth. Active surrogate estimators: An active learning approach to label-efficient model evaluation. *Advances in Neural Information Processing Systems*, 35:24557–24570, 2022. 13
- Alex Krizhevsky, Ilya Sutskever, and Geoffrey E Hinton. Imagenet classification with deep convolutional neural networks. In F. Pereira, C.J. Burges, L. Bottou, and K.Q. Weinberger (eds.), *Advances in Neural Information Processing Systems*, volume 25. Curran Associates, Inc., 2012. URL https://proceedings.neurips.cc/paper_files/paper/2012/file/c399862d3b9d6b76c8436e924a68c45b-Paper.pdf. 24, 25
- Yang Li, Jie Ma, Miguel Ballesteros, Yassine Benajiba, and Graham Horwood. Active evaluation acquisition for efficient LLM benchmarking, 2025. URL <https://openreview.net/forum?id=tKnPtyDt6H>. 13
- Percy Liang, Rishi Bommasani, Tony Lee, Dimitris Tsipras, Dilara Soylu, Michihiro Yasunaga, Yian Zhang, Deepak Narayanan, Yuhuai Wu, Ananya Kumar, et al. Holistic evaluation of language models. *arXiv preprint arXiv:2211.09110*, 2022. 1, 13
- Frederic M Lord and Melvin R Novick. *Statistical theories of mental test scores*. IAP, 2008. 13
- Rupak Majumdar and Filip Nikić. Why is random testing effective for partition tolerance bugs? *Proceedings of the ACM on Programming Languages*, 2(POPL):1–24, 2017. 13
- Leland McInnes, John Healy, and James Melville. Umap: Uniform manifold approximation and projection for dimension reduction, 2020. URL <https://arxiv.org/abs/1802.03426>. 15

- Grégoire Mialon, Clémentine Fourier, Thomas Wolf, Yann LeCun, and Thomas Scialom. Gaia: a benchmark for general ai assistants. In *The Twelfth International Conference on Learning Representations*, 2023. 13
- Yotam Perlitz, Elron Bandel, Ariel Gera, Ofir Arviv, Liat Ein-Dor, Eyal Shnarch, Noam Slonim, Michal Shmueli-Scheuer, and Leshem Choshen. Efficient benchmarking of language models. *arXiv preprint arXiv:2308.11696*, 2023. 13
- Felipe Maia Polo, Lucas Weber, Leshem Choshen, Yuekai Sun, Gongjun Xu, and Mikhail Yurochkin. tinybenchmarks: evaluating LLMs with fewer examples. In *Forty-first International Conference on Machine Learning*, 2024. URL <https://openreview.net/forum?id=qAm13FpfhG>. 2, 3, 5, 6, 7, 13, 15
- Ameya Prabhu, Vishaal Udandara, Philip Torr, Matthias Bethge, Adel Bibi, and Samuel Albanie. Efficient lifelong model evaluation in an era of rapid progress. In *The Thirty-eighth Annual Conference on Neural Information Processing Systems*, 2024. URL <https://openreview.net/forum?id=A7wC1CTkY1>. 24, 25
- Alec Radford, Jeff Wu, Rewon Child, David Luan, Dario Amodei, and Ilya Sutskever. Language models are unsupervised multitask learners. *OpenAI blog*, 2019. 6
- Tim Rädtsch, Leon Mayer, Simon Pavicic, A Emre Kavur, Marcel Knopp, Barış Öztürk, Klaus Maier-Hein, Paul F Jaeger, Fabian Isensee, Annika Reinke, et al. Bridging vision language model (vlm) evaluation gaps with a framework for scalable and cost-effective benchmark generation. *arXiv preprint arXiv:2502.15563*, 2025. 13
- Alexander Rubinstein, Luca Scimeca, Damien Teney, and Seong Joon Oh. Scalable ensemble diversification for ood generalization and detection. *arXiv preprint arXiv:2409.16797*, 2024. 2, 4, 13
- Olga Russakovsky, Jia Deng, Hao Su, Jonathan Krause, Sanjeev Satheesh, Sean Ma, Zhiheng Huang, Andrej Karpathy, Aditya Khosla, Michael Bernstein, Alexander C. Berg, and Li Fei-Fei. Imagenet large scale visual recognition challenge, 2015. URL <https://arxiv.org/abs/1409.0575>. 24
- Keisuke Sakaguchi, Ronan Le Bras, Chandra Bhagavatula, and Yejin Choi. Winogrande: An adversarial winograd schema challenge at scale. *Communications of the ACM*, 64(9):99–106, 2021. 6, 14
- Igal Sason. On reverse pinsker inequalities. *arXiv preprint arXiv:1503.07118*, 2015. 22
- Aarohi Srivastava, Abhinav Rastogi, Abhishek Rao, Abu Awal Md Shoeb, Abubakar Abid, Adam Fisch, Adam R Brown, Adam Santoro, Aditya Gupta, Adrià Garriga-Alonso, et al. Beyond the imitation game: Quantifying and extrapolating the capabilities of language models. *arXiv preprint arXiv:2206.04615*, 2022. 13
- Hugo Touvron, Thibaut Lavril, Gautier Izacard, Xavier Martinet, Marie-Anne Lachaux, Timothée Lacroix, Baptiste Rozière, Naman Goyal, Eric Hambro, Faisal Azhar, Aurelien Rodriguez, Armand Joulin, Edouard Grave, and Guillaume Lample. Llama: Open and efficient foundation language models, 2023. URL <https://arxiv.org/abs/2302.13971>. 6
- Rajan Vivek, Kawin Ethayarajh, Diyi Yang, and Douwe Kiela. Anchor points: Benchmarking models with much fewer examples. *arXiv preprint arXiv:2309.08638*, 2023. 2, 3, 5, 13
- Alex Wang, Amanpreet Singh, Julian Michael, Felix Hill, Omer Levy, and Samuel R Bowman. Glue: A multi-task benchmark and analysis platform for natural language understanding. *arXiv preprint arXiv:1804.07461*, 2018. 1, 13
- Ross Wightman. Pytorch image models. <https://github.com/rwightman/pytorch-image-models>, 2019. 24, 25
- Peiwen Yuan, Yueqi Zhang, Shaoxiong Feng, Yiwei Li, Xinglin Wang, Jiayi Shi, Chuyi Tan, Boyuan Pan, Yao Hu, and Kan Li. Beyond one-size-fits-all: Tailored benchmarks for efficient evaluation. *arXiv preprint arXiv:2502.13576*, 2025. 13

Rowan Zellers, Ari Holtzman, Yonatan Bisk, Ali Farhadi, and Yejin Choi. Hellaswag: Can a machine really finish your sentence? In *Proceedings of the 57th Annual Meeting of the Association for Computational Linguistics*, 2019. 6, 14

Guanhua Zhang, Florian E Dorner, and Moritz Hardt. How benchmark prediction from fewer data misses the mark. *arXiv preprint arXiv:2506.07673*, 2025. 2, 13, 14, 18

Kaichen Zhang, Bo Li, Peiyuan Zhang, Fanyi Pu, Joshua Adrian Cahyono, Kairui Hu, Shuai Liu, Yuanhan Zhang, Jingkang Yang, Chunyuan Li, and Ziwei Liu. Lmms-eval: Reality check on the evaluation of large multimodal models, 2024. URL <https://arxiv.org/abs/2407.12772>. 1, 13

Hongyu Zhao, Ming Li, Lichao Sun, and Tianyi Zhou. Bento: Benchmark task reduction with in-context transferability. *arXiv preprint arXiv:2410.13804*, 2024. 13

DISCLAIMER FOR USE OF LLMs

We primarily used LLMs in coding co-pilot applications to facilitate experimentation and help with plotting code for result presentation. LLMs were also used as writing tools to assist in refining the paper. However, the final version was carefully reviewed and finalized by the authors. No LLMs were used in ideation and experimental design.

A RELATED WORK

We review prior work relevant to our approach. We first highlight the escalating cost of evaluation for contemporary large models and motivate the need for efficiency. We then survey prior attempts at efficient benchmarking, covering instance and task reduction techniques. Finally, we describe our novelty and contributions.

Cost of evaluation. The evaluation of modern large models is currently driven by increasingly sophisticated benchmarks assessing a wide array of capabilities, from the foundational GLUE (Wang et al., 2018) and the comprehensive HELM (Liang et al., 2022) to LMMs-Eval for multimodal models (Zhang et al., 2024), the diverse BIG-bench (Srivastava et al., 2022), Prometheus for measuring diverse LLM capabilities (Kim et al., 2023), and GAIA for general AI assistants (Mialon et al., 2023). This progress comes at an escalating cost: models have grown significantly in size, making each inference step more resource-intensive, while the scaling of test-time computations has dramatically increased the per-task evaluation costs. Furthermore, end-user requirements have diversified to encompass not only output content but also style and manner. Consequently, a single evaluation on modern benchmarks can demand hundreds to thousands of GPU hours. For examples, LMMs-Eval can require between 30 and 1400 hours on $8 \times A100$ GPUs per model (Zhang et al., 2024; Polo et al., 2024), and HELM evaluations can exceed 4000 GPU hours per model (Liang et al., 2022; Polo et al., 2024).

Label-efficient evaluation. In the pre-LLM context, labelling a test set used to be a cost bottleneck for evaluation. In this context, the concept of “active testing” has been explored, where labelling budget is maximally assigned to information-rich samples (Majumdar & Niksic, 2017; Ji et al., 2021; Deng & Zheng, 2021; Kossen et al., 2021; Hu et al., 2023; Kossen et al., 2022; Huang et al., 2024; Fogliato et al., 2024). In our case, we are concerned with the *inference costs* of evaluation. As such, active testing approaches are not directly applicable, as they require a full inference over the test set to identify informative samples to label.

Efficient benchmarking. In the LLM era, benchmarks have diversified to measure multiple capabilities and styles of model behaviours. Researchers have proposed strategies to build an efficient benchmark in the first place (Perlitz et al., 2023; Rädtsch et al., 2025). There were attempts to compress multiple benchmarks, measuring an array of capabilities of LLMs, into a single one by eliminating redundancies (Kipnis et al., 2024; Zhao et al., 2024; Yuan et al., 2025). Others have focused on selection of small, informative subsets, also known as “Anchor point” approaches (Vivek et al., 2023; Polo et al., 2024; Li et al., 2025; Gupta et al., 2025). Given an entire dataset, they compute a small subset of data points according to the *representativeness* criterion, determined through the correctness patterns of a large number of *source models*. Afterwards, the target model performance is estimated based on weighted accuracy computation on the selected subset. In particular, tiny-Benchmarks (Polo et al., 2024) have adopted Item Response Theory (IRT) (Lord & Novick, 2008) to estimate model performance in a principled manner. Hofmann et al. (2025) proposed an IRT-based approach to LLM evaluation that selects anchor points dynamically for each model, guided by its predictions on previously chosen anchors. To address the growing number of methods for efficient LLM evaluation, Zhang et al. (2025) recently introduced a large-scale benchmark. In this work, we adopt approaches from the black-box model analysis techniques, explained below.

Our novelty and contribution. We differentiate our approach, Diversifying Sample Condensation (DISCO), from previous work in two aspects. (1) *model disagreement* (Rubinstein et al., 2024) is a simpler and more effective proxy for sample informativeness than *representativeness* (Vivek et al., 2023; Polo et al., 2024). (2) The application of metamodels on model signatures is a simpler and more effective approach than direct accuracy evaluation approaches (Vivek et al., 2023) or prior approaches that require estimating latent model parameters (Polo et al., 2024; Kipnis et al., 2024).

| Split | Rank | Method | Dims | Rank |
|-----------------|--------------|------------|------------|--------------|
| Chrono. | 0.987 | None | 3100 | 0.918 |
| Uniform | 0.986 | UMAP | 64 | 0.982 |
| (a) Model split | | UMAP | 128 | 0.970 |
| | | UMAP | 256 | 0.970 |
| | | PCA | 32 | 0.983 |
| | | PCA | 64 | 0.987 |
| | | PCA | 128 | 0.987 |
| | | PCA | 256 | 0.987 |
| | | PCA | 300 | 0.985 |

| Strat. | Rank | Method | Rank |
|-----------|--------------|---------------------|--------------|
| Yes | 0.978 | kNN | 0.971 |
| No | 0.987 | Rand. Forest | 0.987 |

| $ \mathcal{F} $ | Rank | Method | Rank |
|-----------------|--------------|---------------|-------|
| 3 | 0.652 | 2-layer MLP | 0.959 |
| 10 | 0.787 | 3-layer MLP | 0.962 |
| 30 | 0.844 | Linear reg. | 0.888 |
| 100 | 0.969 | Ridge reg. | 0.918 |
| 300 | 0.975 | Lasso | 0.908 |
| 382 | 0.987 | Grad boosting | 0.980 |

| Method | Rank |
|---------------------|--------------|
| kNN | 0.971 |
| Rand. Forest | 0.987 |
| 2-layer MLP | 0.959 |
| 3-layer MLP | 0.962 |
| Linear reg. | 0.888 |
| Ridge reg. | 0.918 |
| Lasso | 0.908 |
| Grad boosting | 0.980 |

Figure 6: **Factor analysis for DISCO on MMLU**. Highlighted in bold are the default design choices for DISCO. All comparisons are based on 100 selected samples.

B EXTENDED EXPERIMENTAL SETUP

Datasets. We evaluate DISCO on four widely used language modeling benchmarks:

- Massive Multitask Language Understanding (MMLU) (Hendrycks et al., 2021) question-answering dataset that covers 57 tasks about world knowledge and problem-solving ability.
- HellaSwag (Zellers et al., 2019) dataset that focuses on commonsense natural language inference.
- Winogrande (Sakaguchi et al., 2021): dataset of 273 expert-crafted pronoun resolution problems originally designed to be unsolvable for statistical models.
- (AI2 Reasoning Challenge (ARC)) (Clark et al., 2018): question-answering dataset that contains only natural, grade-school science questions (authored for human tests) and requires knowledge and reasoning.

B.1 FACTOR ANALYSIS (LANGUAGE)

We analyse the impact of several design choices involved in our DISCO on MMLU dataset. See Table 6 for an overview.

Model split. In a recent benchmark for efficient LLM evaluation Zhang et al. (2025), the authors observed that prediction performance drops sharply when test models outperform training models. We extend this idea by replacing performance-based splits with chronological splits, training on older models and testing on newer ones. This better reflects real-world usage, whereas performance-based splits create an artificial stress test.

For this purpose, we introduced the *chronological split* in §4.1. We examine the impact of this model splitting on the result. We observe that our DISCO is robust to the choice of splitting strat-

egy. Chronological splitting yields a rank correlation of .987, which is nearly identical to the .986 obtained with uniform splitting (Table 6 (a)).

Stratification. We measure the efficacy of the stratification strategy in (Polo et al., 2024) where equal numbers of anchor points are selected from each of 57 tasks in MMLU dataset (Table 6 (b)). We find that stratification (.978) is not effective when data points are sampled according to PDS (.987).

Number of source models. We analyse the sensitivity of DISCO to the number of source models $|\mathcal{F}|$ (Table 6 (c)). With only 100 models (.969 rank correlation), it already outperforms TinyBenchmarks, which uses all 382 available source models (.927 in Table 1). As the number of source models increases, rank correlation steadily improves, reaching a maximum of .987 for $|\mathcal{F}| = 382$.

Dimensionality reduction. We compare PCA with different target dimensions to Uniform Manifold Approximation and Projection (UMAP) (McInnes et al., 2020) for dimensionality reduction (Table 6 (d)). We notice that dimensionality reduction helps reduce potential overfitting: without it (using all 3100 dimensions), the correlation is .918, while with PCA at 256 dimensions, it improves to .987. Overall, PCA outperforms UMAP and remains robust across a wide range of dimensions.

Prediction model. We compare a wide range of prediction models (Table 6 (e)). Random Forest achieves the highest rank correlation of .987, outperforming all other methods.

C COMPUTATIONAL COSTS

We report the space–time complexity for the main stages of DISCO, as well as the cost of direct evaluation of a target model. The numbers correspond to a single H100 GPU and are extrapolated from evaluations of five diverse 32B LLMs on MMLU (standard deviation across 5 runs).

C.1 DISCO PIPELINE OVERVIEW

The DISCO pipeline consists of two stages: an **offline** stage (run once) and an **online** stage (run for each new target model).

Offline Stage

- Evaluate M source models on the full test dataset ($M = 385$ in this experiment)
- Store source model outputs
- Select 100 anchor points that maximize PDS/JSD
- Concatenate outputs on anchor points to form model signatures
- Train a predictor to estimate model performance on the full test dataset from these signatures

Online Stage

- Evaluate one target model on the 100 anchor points
- Store target model outputs
- Concatenate to obtain the target model signature
- Run the predictor to estimate performance on the full test dataset

For every target model, the anchor points and predictor trained offline are reused.

C.2 COST METRICS

The majority of compute is required by the offline stage (3284 GPU-hours).

| Metric | Value |
|------------------------------|----------------------------|
| Offline computation cost | 3284.05 ± 592.90 GPU-hours |
| Outputs storage (offline) | 86.54 MB |
| Signatures storage (offline) | 400 KB |
| Online computation cost | 0.07 ± 0.01 GPU-hours |
| Outputs storage (online) | 224.78 KB |
| Signatures storage (online) | 1 KB |
| Direct evaluation cost | 8.53 ± 1.54 GPU-hours |
| Computation savings | 8.46 ± 1.54 GPU-hours |

C.3 BREAK-EVEN ANALYSIS: HOW MANY EVALUATIONS JUSTIFY DISCO SETUP?

DISCO breaks even at **389 evaluations**. Since each DISCO evaluation saves 8.46 GPU-hours per model (vs. 8.53 GPU-hours direct evaluation, minus 0.07 GPU-hours online DISCO cost), the break-even point is:

$$389 = \frac{3284}{8.46}.$$

In practice, hundreds of checkpoint evaluations naturally occur during model development. For example, a single OLMo-2-32B training run includes **753 checkpoints** on Hugging Face, already exceeding break-even.

In some cases, there is no need to evaluate source models at all if offline predictions are downloaded from platforms such as open-llm-leaderboard.

C.4 COMPARISON TO ALTERNATIVE APPROACHES

We briefly remind the pipelines of the compared methods:

- **Selection:** select a set of anchor points, i.e., a subset of the full test dataset based on different signals (random, IRT, model disagreement, etc.).
- **Prediction:** estimate model performance on the full test dataset from outputs on anchor points.

That is why we use “Selection” and “Prediction” columns to explain the difference between methods. See § 3.1 for details on selection methods, and § 3.2 for details on prediction methods.

| Method | Selection | Prediction | Offline (GPU-h) | Online (GPU-s) |
|----------------|---------------------|-------------|-----------------|----------------|
| Baseline | – (use all samples) | Direct eval | – | 30739 ± 5514 |
| Baseline | Random | Direct eval | – | 218 ± 39 |
| tinyBenchmarks | Random | gp-IRT | 3284 ± 592 | 219 ± 39 |
| tinyBenchmarks | Anchor-corr | gp-IRT | 3284 ± 592 | 219 ± 39 |
| tinyBenchmarks | Anchor-IRT | gp-IRT | 3284 ± 592 | 219 ± 39 |
| DISCO | High-PDS | RF | 3284 ± 592 | 218 ± 39 |
| DISCO | High-PDS | KNN | 3284 ± 592 | 218 ± 39 |

The differences in online cost across methods are negligible (e.g., 219 vs. 218 GPU-seconds). Offline costs are equal up to rounding. Efficient evaluation methods allow to save $\frac{(30739-218)}{30739} \cdot 100\% = 99.3\%$ of evaluation cost in comparison to full evaluation.

D QUALITATIVE MEANING OF RANK CORRELATION IMPROVEMENTS

To justify the additional computation required for DISCO relative to direct evaluation, we illustrate how the increase in rank correlation from 91.6 (direct evaluation) to 98.7 (DISCO) in Table 4 translates into qualitative improvements in model ranking.

Figure 7 includes scatter plots of true vs. predicted ranks (see Figure 7). The direct-evaluation predictor demonstrates noticeable spread around the diagonal, while DISCO’s predictions align almost perfectly with it, indicating substantially more reliable ranking.

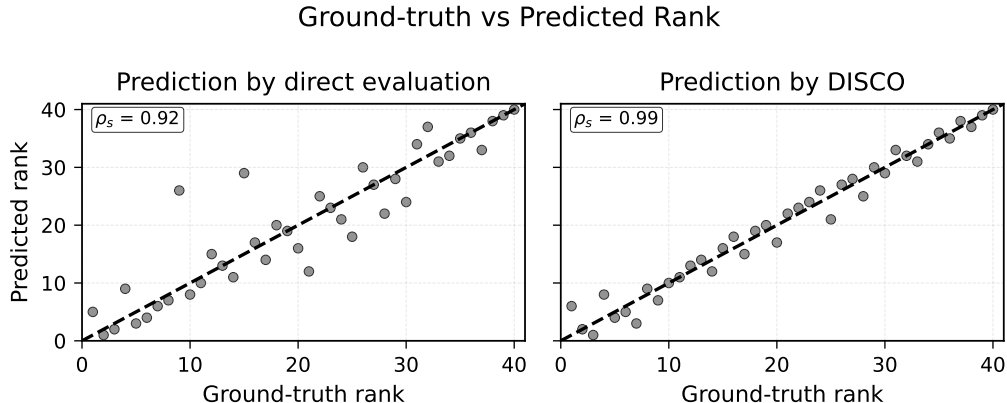


Figure 7: True vs. predicted rank comparison: direct evaluation vs. DISCO. ρ_s means Spearman rank correlation.

E ADDITIONAL EVALUATION RESULTS

E.1 REPORT CONFIDENCE INTERVALS

We report the standard deviation for the previously reported results on MMLU from Table 4, evaluated over one fixed chronological split and 5 independent runs.

We briefly remind the pipelines of the compared methods:

- **Selection:** select a set of anchor points, i.e., a subset of the full test dataset based on different signals (random, IRT, model disagreement, etc.).
- **Prediction:** estimate model performance on the full test dataset from outputs on anchor points.

That is why we use “Selection” and “Prediction” columns to explain the difference between methods. See § 3.1 for details on selection methods, and § 3.2 for details on prediction methods. MAE is mean absolute error; Rank is Spearman rank correlation.

| Method | Selection | Prediction | MAE ↓ | Rank ↑ |
|----------------|-------------|-------------------|-----------------|----------------|
| Baseline | Random | Direct evaluation | 3.45 ± 0.67 | 91.6 ± 2.6 |
| tinyBenchmarks | Random | gp-IRT | 2.79 ± 0.20 | 92.2 ± 2.3 |
| tinyBenchmarks | Anchor-corr | gp-IRT | 2.08 ± 0.20 | 92.7 ± 2.1 |
| tinyBenchmarks | Anchor-IRT | gp-IRT | 3.25 ± 0.49 | 92.2 ± 1.5 |
| DISCO | High JSD | KNN | 1.14 ± 0.00 | 97.5 ± 0.0 |
| DISCO | High JSD | RF | 1.30 ± 0.02 | 98.7 ± 0.1 |
| DISCO | High PDS | KNN | 1.31 ± 0.00 | 97.2 ± 0.0 |
| DISCO | High PDS | RF | 1.07 ± 0.04 | 98.7 ± 0.2 |

DISCO results are more stable than those of IRT and random sampling. This is because the only random component is Random Forest initialization. In contrast, IRT is trained using variational inference, where stochastic gradient optimization introduces additional randomness beyond model parameter initialization.

E.2 MULTIPLE TRAIN/TEST SPLIT FOR CHRONOLOGICAL EVALUATION

To expand the number of chronological splits, we bootstrap 5 different train/test chronological splits using the following protocol: for each run, we split models into 385 old and 40 new based on timestamps, then bootstrap 346 source and 36 test models from these sets. Details on the chronological split can be seen in § 4.1. Results for the new splits can be seen below.

| Method | Selection | Prediction | MAE ↓ | Rank ↑ |
|----------------|-------------|-------------------|-----------------|----------------|
| Baseline | Random | Direct evaluation | 2.85 ± 0.85 | 93.3 ± 3.0 |
| tinyBenchmarks | Random | gp-IRT | 2.42 ± 0.43 | 93.6 ± 2.5 |
| tinyBenchmarks | Anchor-corr | gp-IRT | 1.93 ± 0.31 | 92.9 ± 3.0 |
| tinyBenchmarks | Anchor-IRT | gp-IRT | 3.13 ± 0.33 | 90.2 ± 4.5 |
| DISCO | High PDS | KNN | 1.23 ± 0.09 | 97.0 ± 1.1 |
| DISCO | High PDS | RF | 1.25 ± 0.14 | 98.0 ± 0.6 |

Bootstrapped chronological splits slightly change the mean values (e.g., rank correlation from 98.6 to 98.0 and MAE from 1.06 to 1.25 for DISCO), but they do not alter the superiority of DISCO over other baselines.

F SENSITIVITY OF DISCO TO MODEL CALIBRATION

To evaluate the sensitivity of DISCO to model calibration, we compared the Expected Calibration Error (ECE) of target models with the Mean Absolute Error (MAE) between their true performance and DISCO-predicted performance on MMLU. We observe a Pearson correlation of 0.49 between MAE and ECE, indicating that better-calibrated models lead to more accurate performance (lower MAE) predictions by DISCO.

This phenomenon is explained by the information relationship between confidence and correctness. For a perfectly calibrated model, the mapping between prediction confidence and correctness is deterministic and monotonic, resulting in high mutual information. In contrast, for a highly miscalibrated model (e.g., random guessing or uniformly confident but incorrect), prediction confidence becomes statistically independent of correctness, leading to low mutual information. Consequently, the more calibrated a model is, the more predictive its confidence patterns are of its true performance, and therefore the more informative its signature is for DISCO performance prediction.

The corresponding scatter plot is shown in Figure 8.

During this analysis, we observed that two factors are confounded in calibration metrics: (1) overall confidence level, and (2) how well predictive uncertainty is reflected in confidence. To isolate the effect of overall confidence, we compared MAE with mean prediction confidence separately. We find a Pearson correlation of -0.47 between MAE and mean confidence, suggesting that overall model confidence is the dominant component of ECE that influences DISCO performance.

Figure 9 presents the corresponding scatter plot.

G PERFORMANCE GAP EXPERIMENTS

In addition to source/target model splits discussed in § B.1, we added experiments with a wider performance gap between source and target models to identify potential failure modes for DISCO. Inspired by (Zhang et al., 2025), we introduce a performance split with varying gaps. We sort all models by their average performance and take the top-10% or top-30% (40 or 128 models) as target models, while using the bottom-90% or bottom-50% (385 or 213 models) as source models. The accuracy gap between the weakest target model and the strongest source model is 0.07%p or 8.18%p.

All model splits are summarized in Table 2.

Table 3 reports Spearman rank correlation.

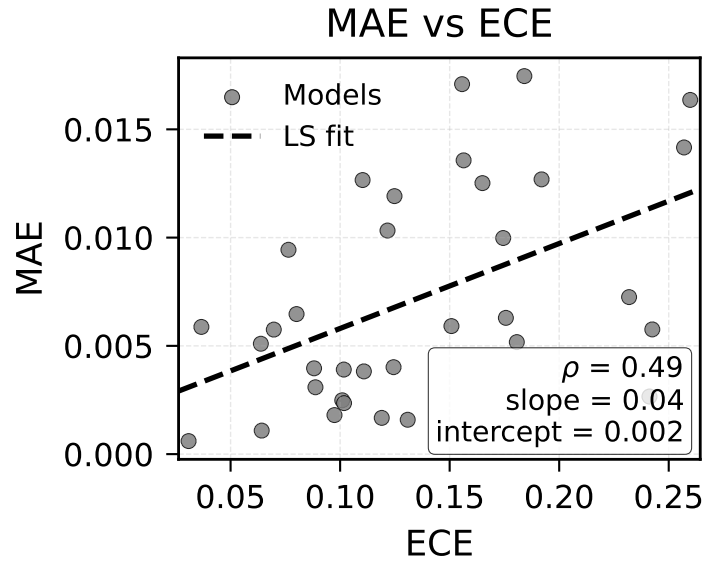


Figure 8: Correlation between DISCO prediction error (MAE) and Expected Calibration Error (ECE).

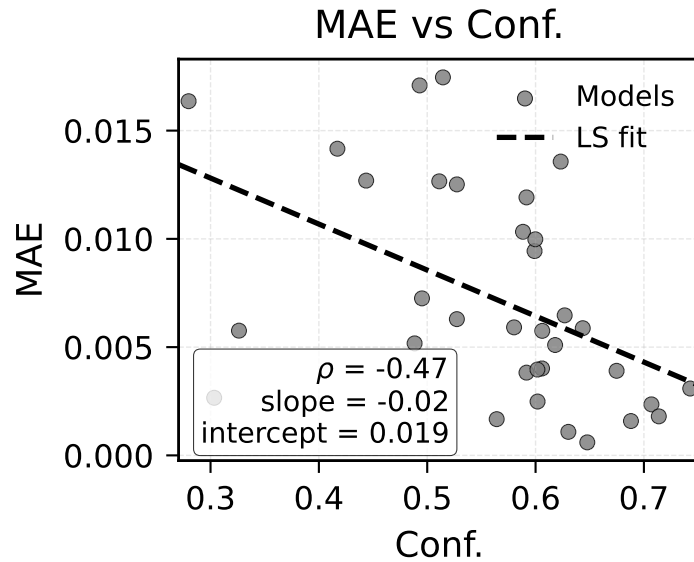


Figure 9: Correlation between DISCO prediction error (MAE) and mean model confidence.

| | IID | Chron. | Performance w/o gap | Perf. w/ gap |
|-----------------------|------------------|---------------|----------------------------|---------------------|
| Prelim. model sorting | – | By timestamp | By performance | By performance |
| Target models | Every 10th model | Top-10% | Top-10% | Top-30% |
| Source models | Everything else | Bottom-90% | Bottom-90% | Bottom-50% |

Table 2: Source/target models splits.

| | IID | Chron. | Perf. w/o gap | Perf. w/ gap |
|---------------------------------------|----------------|----------------|----------------|----------------|
| Direct eval on random subset | 92.1 \pm 1.3 | 91.6 \pm 2.6 | 89.8 \pm 5.9 | 87.4 \pm 5.7 |
| DISCO | 98.6 \pm 0.3 | 98.7 \pm 0.2 | 98.1 \pm 0.2 | 89.2 \pm 1.0 |
| Mean difference (DISCO – direct eval) | +6.5 | +7.1 | +8.7 | +1.8 |

Table 3: DISCO benefit vs direct evaluation on random subset across various source/target models splits.

For a source/target split with a performance gap, the difference between DISCO and direct evaluation is 1.8%p, which is lower than for the IID split (6.5%p), the chronological split (7.1%p), or the performance split without a gap (8.7%p).

While this scenario can be seen as a failure mode for DISCO, we believe that such a source/target performance gap does not happen in practice. Instead, the accuracies of source and target models are often mixed. There are two main reasons for that. First, when practitioners develop new models, their early versions are often worse than the best previously evaluated models. Second, it takes time before new models consistently outperform older ones. Infrequent extra evaluations can allow practitioners to always keep the performance gap low. That makes the performance split with a gap less realistic than other splits. **We thus conclude that DISCO does not break when the source and target model distributions differ, but only when the difference is unrealistically substantial.**

G.1 MUTUAL INFORMATION AND JENSEN-SHANNON DIVERGENCE

In this section, we show that Mutual Information is equivalent to JSD in our setting. We present the setup and assumptions, then prove the proposition.

G.1.1 SETUP.

Let $m \sim \text{Unif}\{1, \dots, M\}$ be the index of a uniformly chosen model. Given m , the prediction on datapoint i has categorical law $P_{\hat{Y}_i|m}$. Define the ensemble mean distribution

$$P_{\hat{Y}_i} = \mathbb{E}_{m \sim \text{Unif}[M]} [P_{\hat{Y}_i|m}] = \frac{1}{M} \sum_{m=1}^M P_{\hat{Y}_i|m}.$$

Let $S(m)$ denote any statistic that is a deterministic function of m computed on \mathcal{D} (e.g. accuracy on \mathcal{D}).

G.1.2 ASSUMPTIONS.

Assumption A1 (Uniform prior). *The model index is uniformly distributed: $m \sim \text{Unif}\{1, \dots, M\}$.*

Assumption A2 (Deterministic predictions). *Conditional on m , each prediction \hat{Y}_i is fully determined by m (or more generally, any residual randomness is independent across i and independent of m).*

G.1.3 PROPOSITION.

Proposition 3. *Under Assumptions A2–A1, if $S(m)$ is injective, then*

$$\text{MI}_{m, \hat{Y}}(S(m); \hat{Y}_i) = \mathcal{H}_{\hat{Y}_i}(P_{\hat{Y}_i}) - \mathbb{E}_{m \sim \text{Unif}[M]} \left[\mathcal{H}_{\hat{Y}_i}(P_{\hat{Y}_i|m}) \right] =: \text{JSD}(\{P_{\hat{Y}_i|m}\}_{m=1}^M).$$

Proof. By Assumption A2 and since $S(m)$ is a deterministic function of m , we have the Markov chain

$$\hat{Y}_i \longleftrightarrow m \longleftrightarrow S(m).$$

If S is injective, then m is recoverable from $S(m)$, hence

$$I(S(m); \hat{Y}_i) = I(m; \hat{Y}_i).$$

By the definition of mutual information,

$$I(m; \hat{Y}_i) = \mathcal{H}_{\hat{Y}_i}(P_{\hat{Y}_i}) - \mathbb{E}_m \left[\mathcal{H}_{\hat{Y}_i}(P_{\hat{Y}_i|m}) \right].$$

Marginal distribution (using Assumption A1):

$$P_{\hat{Y}_i} = \sum_{m=1}^M \Pr(m) P_{\hat{Y}_i|m} = \frac{1}{M} \sum_{m=1}^M P_{\hat{Y}_i|m}.$$

Thus $\mathcal{H}_{\hat{Y}_i}(P_{\hat{Y}_i})$ is the entropy of the mixture distribution.

Conditional entropy (using Assumption A1):

$$\mathbb{E}_m \left[\mathcal{H}_{\hat{Y}_i}(P_{\hat{Y}_i|m}) \right] = \frac{1}{M} \sum_{m=1}^M \mathcal{H}_{\hat{Y}_i}(P_{\hat{Y}_i|m}).$$

Combine:

$$I(m; \hat{Y}_i) = \mathcal{H}_{\hat{Y}_i}(P_{\hat{Y}_i}) - \frac{1}{M} \sum_{m=1}^M \mathcal{H}_{\hat{Y}_i}(P_{\hat{Y}_i|m}) =: \text{JSD}(\{P_{\hat{Y}_i|m}\}_{m=1}^M).$$

□

H BOUNDS FOR JENSEN-SHANNON DIVERGENCE (JSD) VIA PREDICTIVE DIVERSITY SCORE (PDS)

In this section, we show that JSD is bounded quadratically below and linearly above by PDS. We first relate JSD to total variation (§ H.1), then show total variation is monotone in PDS (§ H.2), and then combine these results in § H.3.

H.1 BOUNDS FOR JSD VIA TOTAL VARIATION (TV)

We begin by showing that JSD is bounded quadratically below and linearly above by total variation. We first introduce the setup with required definitions (§ H.1.1), then prove the proposition (§ H.1.2).

H.1.1 SETUP.

Let $\{P_{\hat{Y}_i|m}\}_{m=1}^M$ be distributions on K classes. Define the mixture

$$\bar{P} = \frac{1}{M} \sum_{m=1}^M P_{\hat{Y}_i|m}.$$

Definition 1 (Jensen–Shannon divergence).

$$\text{JSD}(\{P_{\hat{Y}_i|m}\}) = \frac{1}{M} \sum_{m=1}^M D_{\text{KL}}(P_{\hat{Y}_i|m} \| \bar{P}) = \mathcal{H}(\bar{P}) - \frac{1}{M} \sum_{m=1}^M \mathcal{H}(P_{\hat{Y}_i|m}).$$

Definition 2 (Total variation). *For distributions P, Q on the same support,*

$$\text{TV}(P, Q) = \frac{1}{2} \|P - Q\|_1.$$

H.1.2 PROPOSITION.

Now, we show that JSD is bounded quadratically below and linearly above by total variation.

Proposition 4 (JSD–TV sandwich bounds). *For any $M \geq 2$ distributions $\{P_{\hat{Y}_i|m}\}_{m=1}^M$ with mixture \bar{P} ,*

$$\frac{2}{\ln 2} \cdot \frac{1}{M} \sum_{m=1}^M \text{TV}(P_{\hat{Y}_i|m}, \bar{P})^2 \leq \text{JSD}(\{P_{\hat{Y}_i|m}\}_{m=1}^M) \leq \frac{M}{M-1} \log M \cdot \frac{1}{M} \sum_{m=1}^M \text{TV}(P_{\hat{Y}_i|m}, \bar{P}).$$

Proof. Lower bound. By Pinsker’s inequality (e.g. Equation 1 in (Sason, 2015)),

$$D_{\text{KL}}(P\|Q) \geq \frac{2}{\ln 2} \text{TV}(P, Q)^2.$$

Substituting $Q = \bar{P}$ and averaging over m yields the lower bound.

Upper bound. Fix m . Write

$$\bar{P} = \alpha P_{\hat{Y}_i|m} + (1 - \alpha)\zeta, \quad \alpha = \frac{1}{M}, \quad \zeta = \frac{1}{M-1} \sum_{s \neq m} P_{\hat{Y}_i|s}.$$

Define $t(i) = \zeta(i)/P_{\hat{Y}_i|m}(i)$ when $P_{\hat{Y}_i|m}(i) > 0$ (set $t(i) = +\infty$ if $P_{\hat{Y}_i|m}(i) = 0, \zeta(i) > 0$). Then $\mathbb{E}_{P_{\hat{Y}_i|m}}[t] = 1$ and

$$D_{\text{KL}}(P_{\hat{Y}_i|m}\|\bar{P}) = \mathbb{E}_{P_{\hat{Y}_i|m}}[-\log(\alpha + (1 - \alpha)t)].$$

Let $f(u) = -\log(\alpha + (1 - \alpha)u)$, $u \geq 0$. Then f is convex, decreasing, with $f(1) = 0$, $f(0) = \log(1/\alpha) = \log M$. By convexity,

$$f(u) \leq (1 - u)f(0) = (1 - u) \log M.$$

Thus,

$$D_{\text{KL}}(P_{\hat{Y}_i|m}\|\bar{P}) \leq \log M \cdot \mathbb{E}_{P_{\hat{Y}_i|m}}[(1 - t)] \leq \log M \cdot \mathbb{E}_{P_{\hat{Y}_i|m}}[(1 - t)_+].$$

Now

$$\mathbb{E}_{P_{\hat{Y}_i|m}}[(1 - t)_+] = \sum_i P_{\hat{Y}_i|m}(i) \max\{0, 1 - \zeta(i)/P_{\hat{Y}_i|m}(i)\} = \sum_i (P_{\hat{Y}_i|m}(i) - \zeta(i))_+.$$

By the balance-of-deviations identity (§ 1),

$$\sum_i (P_{\hat{Y}_i|m}(i) - \zeta(i))_+ = \text{TV}(P_{\hat{Y}_i|m}, \zeta).$$

Finally, since $\bar{P} = \alpha P_{\hat{Y}_i|m} + (1 - \alpha)\zeta$, one has

$$\text{TV}(P_{\hat{Y}_i|m}, \zeta) = \frac{M}{M-1} \text{TV}(P_{\hat{Y}_i|m}, \bar{P}).$$

Combining yields

$$D_{\text{KL}}(P_{\hat{Y}_i|m}\|\bar{P}) \leq \frac{M}{M-1} \log M \cdot \text{TV}(P_{\hat{Y}_i|m}, \bar{P}).$$

Averaging over m gives the upper bound. \square

Remark 1. *The lower bound is quadratic in total variation, the upper bound linear. Thus, JSD interpolates between quadratic growth near equality and linear growth in worst-case separation.*

H.2 BOUNDS FOR TOTAL VARIATION VIA PREDICTIVE DIVERSITY SCORE

We next show that total variation is monotone in PDS. We introduce the setup with definitions and lemmas (§ H.2.1), then prove the proposition (§ H.2.2).

H.2.1 SETUP.

Fix a class c . Let $X_m = P_{\hat{Y}_i|m}(c)$ and $\mu = \bar{P}(c)$. Define:

Definition 3 (Envelope and spread, per class).

$$E_c = \max_m X_m - \mu, \quad U_c = \frac{1}{2M} \sum_{m=1}^M |X_m - \mu|.$$

Definition 4 (Predictive Diversity Score).

$$\text{PDS}(\{P_{\hat{Y}_i|m}\}) = \sum_{c=1}^K \max_m P_{\hat{Y}_i|m}(c).$$

Lemma 1 (Balance-of-deviations identity). *For any a_1, \dots, a_M with $\sum_m a_m = 0$, writing $a_+ = \max\{0, a\}$,*

$$\sum_{m=1}^M (a_m)_+ = \sum_{m=1}^M (a_m)_- = \frac{1}{2} \sum_{m=1}^M |a_m|.$$

Proof. Decompose $a = a_+ - a_-$, $|a| = a_+ + a_-$. Summing and using $\sum_m a_m = 0$ gives

$$\sum_m a_{m,+} - \sum_m a_{m,-} = 0 \quad \Rightarrow \quad \sum_m a_{m,+} = \sum_m a_{m,-}.$$

Then

$$\sum_m |a_m| = \sum_m (a_{m,+} + a_{m,-}) = 2 \sum_m a_{m,+}.$$

□

Applying Lemma 1 with $a_m = X_m - \mu$ yields

$$U_c = \frac{1}{M} \sum_{m: X_m > \mu} (X_m - \mu).$$

H.2.2 PROPOSITION.

Now, we show that total variation is monotone in PDS.

Proposition 5 (Spread–envelope bounds). *Use notation from Appendix H.2.1. For each class c , if at most z models satisfy $X_m > \mu$, then*

$$\frac{1}{M} E_c \leq U_c \leq \frac{z}{M} E_c.$$

Aggregating over classes,

$$\frac{1}{M} E \leq U \leq \frac{z}{M} E,$$

where

$$E = \sum_{c=1}^K E_c, \quad U = \sum_{c=1}^K U_c = \frac{1}{M} \sum_{m=1}^M \text{TV}(P_{\hat{Y}_i|m}, \bar{P}).$$

Proof. If $E_c = 0$, then $X_m = \mu$ for all m so $U_c = 0$. Otherwise, let $m^* = \arg \max_m X_m$. Then

$$U_c = \frac{1}{M} \sum_{m: X_m > \mu} (X_m - \mu) \geq \frac{1}{M} (X_{m^*} - \mu) = \frac{1}{M} E_c.$$

For the upper bound, each positive term is at most E_c , and there are at most z such terms, hence

$$U_c \leq \frac{z}{M} E_c.$$

Summing over classes gives the aggregated bound. □

H.3 FINAL SANDWICH INEQUALITY

Finally, we combine results from § H.1.1 and § H.2 to show that JSD is bounded quadratically below and linearly above by PDS.

Proposition 6 (JSD–PDS sandwich). *Use notation from Proposition 1.*

$$\frac{2}{M^2 \ln 2} (\text{PDS}(\{P_{\hat{Y}_i|m}\}) - 1)^2 \leq \text{JSD}(\{P_{\hat{Y}_i|m}\}) \leq \frac{M}{M-1} \log M \cdot (\text{PDS}(\{P_{\hat{Y}_i|m}\}) - 1).$$

Proof. From Theorem 4,

$$\text{JSD} \geq \frac{2}{\ln 2} U^2, \quad \text{JSD} \leq \frac{M}{M-1} \log M \cdot U.$$

Define

$$E := \sum_{c=1}^K E_c, \quad U := \sum_{c=1}^K U_c.$$

By the definitions,

$$U = \sum_{c=1}^K \frac{1}{2M} \sum_{m=1}^M |P_{\hat{Y}_i|m}(c) - \bar{P}(c)| := \frac{1}{2M} \sum_{m=1}^M \|P_{\hat{Y}_i|m} - \bar{P}\|_1 := \frac{1}{M} \sum_{m=1}^M \text{TV}(P_{\hat{Y}_i|m}, \bar{P}),$$

where $\bar{P} = P_{\hat{Y}_i} = \frac{1}{M} \sum_{m=1}^M P_{\hat{Y}_i|m}$, and

$$E = \sum_{c=1}^K \left(\max_m P_{\hat{Y}_i|m}(c) - \bar{P}(c) \right) = \text{PDS} - 1.$$

From Proposition 5,

$$\frac{1}{M}(\text{PDS} - 1) \leq U \leq \frac{z}{M}(\text{PDS} - 1).$$

Combining and noticing that $1 \leq z \leq M$ yields the quadratic lower bound and linear upper bound in $(\text{PDS} - 1)$. \square

I VISION RESULTS

We introduce the setup (§I.1), describe baselines (§I.2), and present results (§I.3).

I.1 SETUP

Dataset. We use ImageNet-1k (Russakovsky et al., 2015) with 1.28 million images. **Models.** We consider 400 models from `timm` (Wightman, 2019) that are pretrained on ImageNet. The models cover convolutional (Krizhevsky et al., 2012) and transformer (Dosovitskiy et al., 2021) architectures. Model sizes range from 0.3M to 300M parameters.

Model Split. As in the language domain (§ 4.1), we use the *chronological split*. The cutoff date is 5 April 2023. The train-test ratio of models is 88:12.

Metrics. We use mean absolute error (MAE) and Spearman rank correlation between the true and predicted performances.

Evaluation. Evaluation protocol follows the one in § 4.1

I.2 ABOUT BASELINES FOR VISION DOMAIN

Our work is not the first to propose efficient evaluation in the vision domain. The two closest methods are Lifelong Benchmark (Prabhu et al., 2024) (NeurIPS 2024) and SSEPY (Fogliato et al., 2024) (ECCV 2024). They propose efficient evaluation methods for visual models, using a similar two-stage framework for efficient evaluation in the language domain (see § 3 / Figure 2 of our submission):

1. Select “important/representative” anchor points.
2. Estimate model performance based on model outputs on the anchor points.

In (Prabhu et al., 2024), mean correctness scores across source models are used to measure sample difficulty, and anchor points are selected by sampling every k -th datapoint after sorting them by difficulty (where $k = \frac{\#\text{all datapoints}}{\#\text{anchor points}}$). Final performance is predicted as a weighted sum of correctness scores predicted for each test datapoint. Predicted correctness scores are binary values indicating relative position (after sorting by difficulty) to the hardest anchor point the target model got right. In (Fogliato et al., 2024), confidence scores of the target model are used to measure sample difficulty. Then samples are clustered by difficulty with K-Means, and anchor points are selected as the centroids of the clusters. Final performance is predicted as a weighted sum of anchor correctness

| Approach | Selection | Prediction | IN val (50k) | |
|-----------------|---------------------|--------------|--------------|--------------|
| | | | §3.1 | §3.2 |
| | | | MAE↓ | Rank↑ |
| Baseline | Random | Direct eval. | 3.03 | 0.652 |
| Lifelong Bench. | Uniform correctness | Weighted sum | 2.06 | 0.838 |
| SSEPY | Uniform confidence | Weighted sum | 3.05 | 0.762 |
| Model signature | Random | Sig. + kNN | 1.72 | 0.808 |
| | | Sig. + RF | 0.86 | 0.944 |
| DISCO (ours) | High PDS | Sig. + kNN | 1.68 | 0.819 |
| | | Sig. + RF | 0.63 | 0.969 |

Table 4: **DISCO compression of ImageNet validation dataset.** We reduce the test set to 100 anchor points. MAE is %p difference in accuracy; Rank is Spearman rank correlation. (1) Model signature is an effective strategy; (2) PDS on top improves further.

scores. Weights for the weighted sum are determined based on the corresponding cluster sizes using Horvitz-Thompson estimator.

The main message of our paper is that for selecting anchor points for efficient evaluation, it is better to select **diversity-inducing data points** (DISCO) than to **make a good coverage of sample difficulty** (prior work). In § 4.2, we have shown that our approach beats prior approaches in the language domain.

Likewise, in the vision domain, the existing approaches (Prabhu et al., 2024; Fogliato et al., 2024) focus on a good coverage of sample difficulty rather than on maximizing per-sample information by seeking diversity-inducing data points. We test empirically in Table 4 whether the same conclusion holds in the vision domain by comparing DISCO to (Prabhu et al., 2024; Fogliato et al., 2024).

We computed the results for these baselines ourselves, as the papers do not contain results on ImageNet. For fair comparison, we use the same setup as described in § I.1.

I.3 MAIN RESULTS

We give an overview of DISCO applied to the vision domain. We use ImageNet-1k with 1.28M images and 400 pretrained models from `timm` (Wightman, 2019), spanning convolutional (Krizhevsky et al., 2012) and transformer (Dosovitskiy et al., 2021) architectures (0.3M–300M parameters). We adopt a *chronological split* with cutoff 5 April 2023 (88:12 train–test). Table 4 summarizes the main results.

Our DISCO approach significantly compresses the ImageNet validation set to 100 data points (99.8% inference cost reduction). With uniform random sampling and Random Forest on model signatures we achieve 0.86%p MAE and .944 rank correlation; with PDS selection and RF, 0.63%p MAE and .969 rank correlation. DISCO (0.969/0.63) outperforms Lifelong Bench. (Prabhu et al., 2024) (0.838/2.06) and SSEPY (Fogliato et al., 2024) (0.762/3.05). The conclusion from language experiments holds: focus on **selecting points on which models typically disagree** rather than wide coverage of sample difficulty.

To illustrate how well the estimated performances align with the true values, we present a scatter plot in Figure 10. The high Pearson correlation coefficient of .970 indicates a strong agreement between the two.

Figure 11 shows performance across varying levels of test set reduction. The relative ranking of evaluation methods remains largely stable, except for the kNN predictor, which degrades as the number of anchor points increases. Notably, DISCO consistently outperforms all baselines, even under extreme compression with as few as 10 samples.

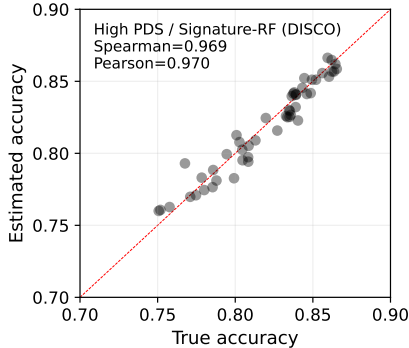


Figure 10: **True and estimated accuracy on ImageNet for 50 models.**

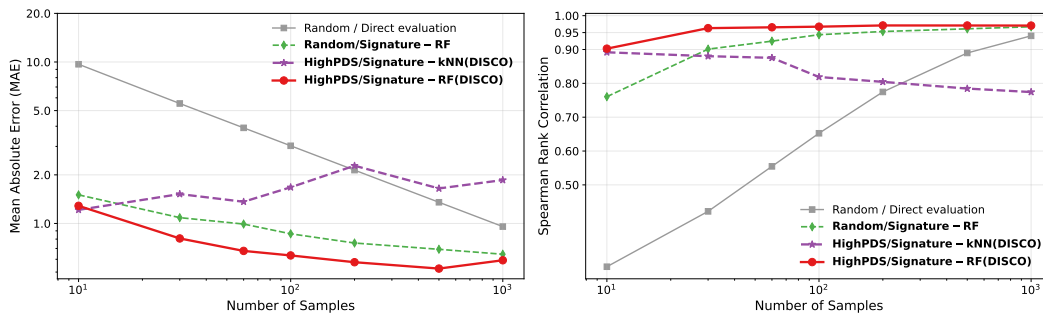


Figure 11: **ImageNet performance estimation vs. compression rates.** Mean absolute error (MAE), measured in %p difference in accuracy, and the Spearman rank correlation between the true model ranking and the estimated model ranking are shown. At 100 samples, the results are identical to Table 4. **Main observations:** Same as for language experiments DISCO hits a better efficiency-precision trade-off across all range of compression rates.